Optimization of Internally Finned Tubes for Solar Receivers

JE Hoffman

Dept. of Mechanical and Mechatronic Engineering, University of Stellenbosch, Private Bag X1, Matieland, 6702, South Africa; Phone: +27 21 808 3554; Fax: + 27 86 615 5206; E-mail: hoffmaj@sun.ac.za

Abstract

SUNSPOT proposes a gas turbine cycle with air as working fluid. Although freely available, air is a poor heat transfer fluid. Metals are the preferred choice for the receiver, as they are relatively cheap and easy to machine. High heat fluxes from the heliostat field will result in high material temperatures, and possible tube failures. This paper explores heat transfer enhancement through triangular fins on the inside of the receiver tubes. The internal heat transfer in the receiver tube depends on the tube diameter, wall thickness, number of fins, gap between fins and helical angle for a fixed flow velocity and tube material. Computational fluid dynamics were used to evaluate the target function and its gradient. The bulk of the heat is transferred by convection to the working fluid. The tube loses heat to the environment through thermal radiation. The optimization routine of choice use sequential convex quadratic approximates of the target function. Preliminary results for a steel tube indicate that the maximum metal temperature can be reduced substantially. Rather high temperature differences across the tube suggest that thermal stresses may be significant.

Key words: solar receiver, air, CFD, optimization

1. Introduction

The SUNSPOT cycle [1] use an air standard open loop Brayton cycle during the day, and a dry-cooled Rankine cycle during the night. Waste heat from the gas turbine outlet is stored in a rock bed during the day, and heat is extracted from the bed during the night to drive the Rankine cycle.

A high turbine inlet temperature is required to increase the power output of the turbine, and also to have sufficient energy left in the air leaving the turbine to charge the rock bed. The bulk of the energy required to raise the air temperature upstream of the turbine should come from concentrated sunlight. A target of temperatures above 800 °C is currently set for the receiver.

The receiver is situated on top of a reasonably tall (~ 100 m) tower, hence designers aim for a fairly compact design. As a result, highly concentrated (~ 300 ×) sunlight is focused onto the receiver. Air is a poor heat transfer fluid, thus the high heat fluxes (~ 300 kW/m^2) in the receiver invariable lead to large temperature differences between the receiver surfaces and the air. As a result, radiation losses are high, but more significantly, material temperatures may exceed design limits.

One way of countering the high temperatures is enhancing the heat transfer on the air side. In a simple tubular receiver [2], this can be achieved by internal fins. It is expected that enhanced heat transfer will come at a cost of an increase in pressure drop across the receiver. Since the receiver is situated between the compressor and turbine, increasing the pressure drop will reduce the overall thermal efficiency of the Brayton cycle. Hence, it becomes an optimization problem.

Kim, Jansen and Jensen [3] did a similar study for short fins (fin height less than 5 % of tube diameter), assuming incompressible, fully developed turbulent, periodic flow with constant properties. Their Reynolds numbers were an order of magnitude higher than the Reynolds numbers reported here. They assumed a constant temperature wall in their model. They reported Nusselt numbers and pressure drops about double that for smooth tubes.

Optimization of tube design was identified as a potential masters' project. It is envisaged to use computational fluid dynamics (CFD) and finite element methods (FEM) for all flow, heat transfer and thermal stress calculations. A prototype of only the final design should be tested to validate the calculations. This paper reports on early attempts to determine the scope of such a project.

Minimize the material temperature of an externally heated, internally finned tube, using triangular fins. Design variables are tube diameter *D*, gap width between fins *w*, the number of fins *N*, tube wall thickness *t*, and fin helical angle θ. Arbitrary bounds are placed on all the design variables. The fin base width is arbitrarily constrained to 0.4 mm, about the thickness of a corrugated sheet.

No attempt was made to calculate the thermal stresses in the tube. The pressure drop was recorded, but played no role in the optimization process.

2. Optimization

The task at hand is to minimize the maximum temperature of the tube material

$$f(\vec{x}) = T(D^*, w^*, N^*, t^*, \theta^*)$$

subject to the constraint

$$g(\vec{x}) = 0.4N + Nw - \pi D \leq 0$$

for

$$\begin{gathered} 15\,mm \leq D \leq 60\,mm \\ 0.5\,mm \leq w \leq 5\,mm \\ 18 \leq N \leq 60 \\ 1.5\,mm \leq t \leq 6\,mm \\ 0° \leq \theta \leq 45° \end{gathered}$$

The design variables were made non-dimensional by dividing each variable by its maximum range.

Newton's method basically searches in the direction of steepest descend, but take curvature of the target function into account [4]. It was tested with excellent results on a few analytic functions.

$$\vec{x}_{k+1} = \vec{x}_k - \frac{\nabla f(\vec{x}_k)}{H(\vec{x}_k)}$$

Evaluation of the Hessian matrix involves second derivatives, calling in the case of 5 design variables for 11 CFD simulations per iteration. Finite differences are used to evaluate the derivatives. Perturbations of 1 % of the range of each (continuous) design variable were arbitrarily chosen for calculating the derivatives. No attempt was made to find the best values for the perturbations that would avoid noise without compromising the accuracy of the result.

Snyman and Hay [5] suggested the use of spherical quadratic functions to approximate the target function. The Hessian is thus replaced with the curvature of the quadratic function

$$H(\vec{x}_k) \approx C_k = \frac{2\{f(\vec{x}_{k-1}) - f(\vec{x}_k) - \nabla^T f(\vec{x}_k)(\vec{x}_{k-1} - \vec{x}_k)\}}{[\![\vec{x}_{k-1} - \vec{x}_k]\!]^2} \quad \ldots (1)$$

This reduces the number of function evaluations (CFD simulations) to 6. Groenwold, Etman and Wood [6] insisted on convex spherical quadratic approximations.

$$C_k = max[C_k^*, a]$$

where C_k^* is calculated from equation (1), and a is a positive real number. This is a sensible approach, since a negative C_k will lead to a maximum, rather than a minimum of the target function. Groenwold, Etman and Wood [6] suggested a = 0.1. In this particular study, C_k^* was initially positive, but switched sign near the optimum. This resulted in rather large changes to the design variables, when small changes were required. Consequently, a revised curvature

$$C_k = |C_k^*|$$

was boldly adopted near the optimum solution. This wasn't tested for any other target functions, so the approach should be used with caution.

If any design variable persistently hit the limit of its range, its value was fixed to the limiting value and it plays no further role in the optimization. However, its gradient was still monitored to confirm that its gradient still want to drive it out of the permissible range. It was allowed back, if its gradient changes sign.

3. CFD Model

Only a 30 mm long section of the internally finned receiver tube was modeled. Although the model would be sensitive to inlet effects, it allows a nearly mesh independent solution on a Stellenbosch University standard issue laptop/desktop (Intel i7 processor and 4 GB RAM). All simulations were done using ANSYS Fluent version 14.0. It was assumed that the tube and fins were made from the same material (mild steel), and that there wasn't a contact resistance between the fins and the tube.

The tube is heated directly from the top by 300 suns. The heat flux at the tube walls is calculated from

$$q''_w = \begin{cases} -\vec{I} \cdot d\vec{A} - \sigma\varepsilon\left|d\vec{A}\right|T_w^4 & if\ the\ area\ element\ faces\ the\ sun \\ -\sigma\varepsilon\left|d\vec{A}\right|T_w^4 & if\ the\ area\ element\ is\ in\ the\ shade \end{cases}$$

Taking the characteristic time of the tube as

$$\tau = \frac{\rho C V}{hA}$$

the response of the tube is fast (~ 24 seconds) relative to the diurnal cycle, and the problem was modeled in the steady state.

The air was modeled as an ideal gas with temperature dependent properties. All air properties were approximated by fitting polynomials through the data of Holman [7]. User defined functions were written for the air viscosity and thermal conductivity, whilst a scheme file was used to enter the specific heat (ANSYS Fluent specific requirement). It was assumes that atmospheric air is delivered to the receiver by a compressor with a pressure ratio of 10 and an isentropic efficiency of 89 %. Thus, the air entering the receiver is at 1 MPa, 603 K. The air inlet velocity was arbitrarily set to 5 m/s. The operating pressure was set to 1 MPa.

Assuming a uniform velocity of 5 m/s at the inlet, the Reynolds number for flow between fins is

$$Re = \frac{\rho V t}{\mu} \approx \frac{5.78\ kg/m^3 \times 5\ m/s \times 0.001\ m}{3.018\ \times 10^{-5}\ kg/ms} = 957$$

This would suggest that the flow in the area of interest is probably laminar[1], hence the flow through the entire domain was modeled as laminar. Based on the hydraulic diameter, the Reynolds number is about 1 900 for the initial design, uncomfortably close to the transitional range.

Thermal radiation was not taken into account on the inside of the tube, despite the relatively high temperatures that were predicted on solid surfaces. The high aspect ratio of the gap between fins, and the small temperature difference across the gap should limit its contribution, and the additional expense of including thermal radiation isn't justified. It is expected that thermal radiation should reduce the maximum tube temperature slightly.

Second order upwind differencing [8] were used for all flow variables.

[1] According to White [9], the flow between flat plates usually become unstable for Reynolds numbers above 1 000. During optimization, the gap size decreased, and the Reynolds number should remain below this limit.

A predominantly hexahedral mesh was constructed, working outwards from the rectangular gaps between the fins. The cell aspect ratio was limited to 2 in the direction of the fin height, and 3 in the flow direction. A triangular mesh was constructed on a cross section through the triangular fins, and this mesh was extruded in the flow direction. A tetrahedral mesh was used for the core of the tube. The mesh at the inlet of the tube is shown in figure 1.

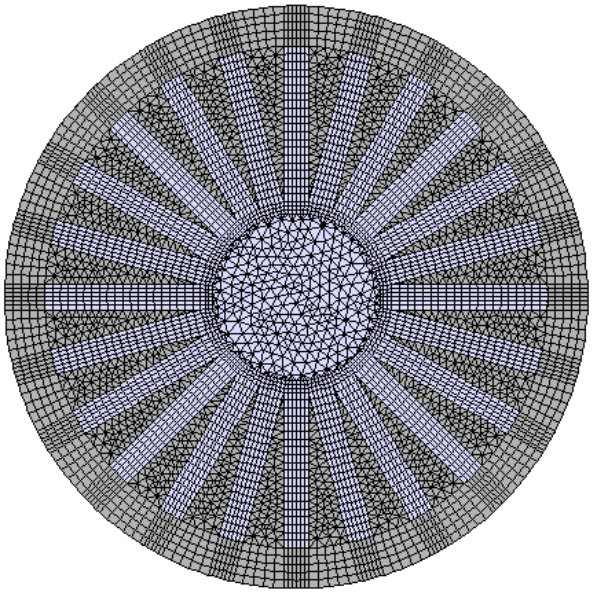

Figure 1. Coarse mesh, viewed from the inlet.

Three meshes, each having twice the number of cells of its predecessor, were constructed to test for mesh independence. Starting from the coarse mesh, cell sizes were varied in all three directions according to the scheme

$$\Delta x_i^j = \frac{\Delta x_i^{j-1}}{\sqrt[3]{2}}$$

The mesh independence test was only performed for the initial geometry. The maximum steel temperatures for the three meshes are given in table 1.

	Cell Count	Pressure Drop [Pa]	Max Metal Temp [K]
Coarse mesh	758 836	122.3	804.48
Medium mesh	1 497 987	129.6	805.00
Fine mesh	2 967 501	132.9	805.40

Table 1 Mesh independence test result.

The discretization error is reducing for both temperature and pressure drop. The rate of error reduction in the case of the temperature is close to the r^{-p} relationship one would expect for asymptotic convergence of a second order scheme. A fourth mesh is required to formally prove mesh independence [10], but this is beyond the typical hardware capability available to students. Taking changes in both temperature and pressure drop with mesh refinement into account, all subsequent simulations were performed on the finest mesh.

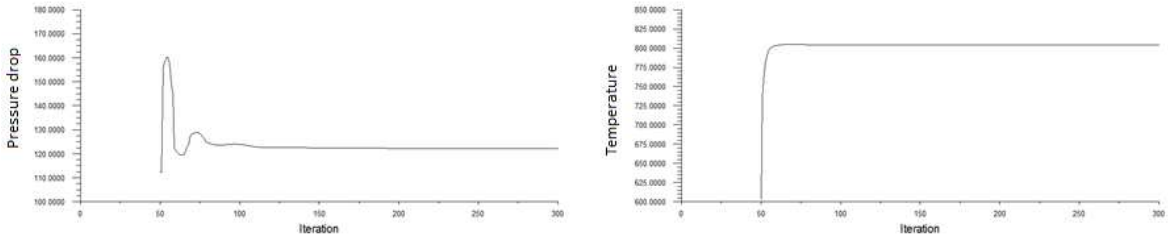

Figure 2. Iterative convergence of pressure drop and maximum temperature.

An additional simulation, using the shear stress transport k-ω model was done as check. The pressure drop was within 0.5 Pa of the laminar result, but the maximum temperature was 18 K lower. One would expect from the Reynolds analogy [9] for compressible flow

$$\frac{C_f}{St} = 2Pr^{2/3}$$

that the heat transfer coefficient for the laminar and turbulent cases would be the same, since the friction factors are the same. A possible explanation may be that the pressure drop is mainly due to the continuous change in flow direction, whilst heat transfer is truly a boundary layer effect. During the optimization process, the gap width, and with it the hydraulic diameter were driven down, hence the flow should recede deeper into the laminar regime. Further simulations all assumed laminar flow.

Residuals converge to Fluent default settings (10^{-3}) relatively quickly, and continue to decrease steadily. The simulations was only judged fully converged when the pressure at the inlet, and the maximum metal temperature do not change for at least 50 iterations. Since the (relative) pressure at the outlet boundary is set to 0 Pa, the pressure at the inlet equates to the pressure drop across the domain.

4. Discussion of results

The design was initialized with the following set

$$\vec{x}_0 = (D_0, w_0, N_0, t_0, \theta_0) = (20mm, 1mm, 24, 1.6mm, 30°)$$

Figure 3 shows the expected temperature profile on solid surfaces for the initial design. The highest temperature is on the side facing the sun, and the temperature increases in the flow direction as the air temperature increase and the velocity profile develops. The temperature profile is slightly rotated anti-clockwise, as cooler air is moved towards the heated surface by the spiraling fins.

Less than half the fins are heated significantly above the air temperature. The side of the tube facing the heliostats is much hotter than the side shaded from the heliostats. The large temperature difference across the tube suggests that thermal stresses and tube deformation might be significant. No attempt was made to solve for the thermal stresses in this work.

The fins induce a strong swirling flow in the open core of the tube, as shown in figure 4. The lowest velocities are at the radius of the fin tips. Although the maximum velocity in the core is about twice the inlet velocity, the velocity profile is box shaped, indicating that the velocity profile is not fully developed yet. The highest air temperatures are recorded in the gaps between the fins. This should result in a higher flow resistance, since the flow accelerates, and the viscosity increases. However, this is dominated by the centrifugal force, and the flow in the gaps is towards the tube wall. Apparently, no flow is directed out of the gaps.

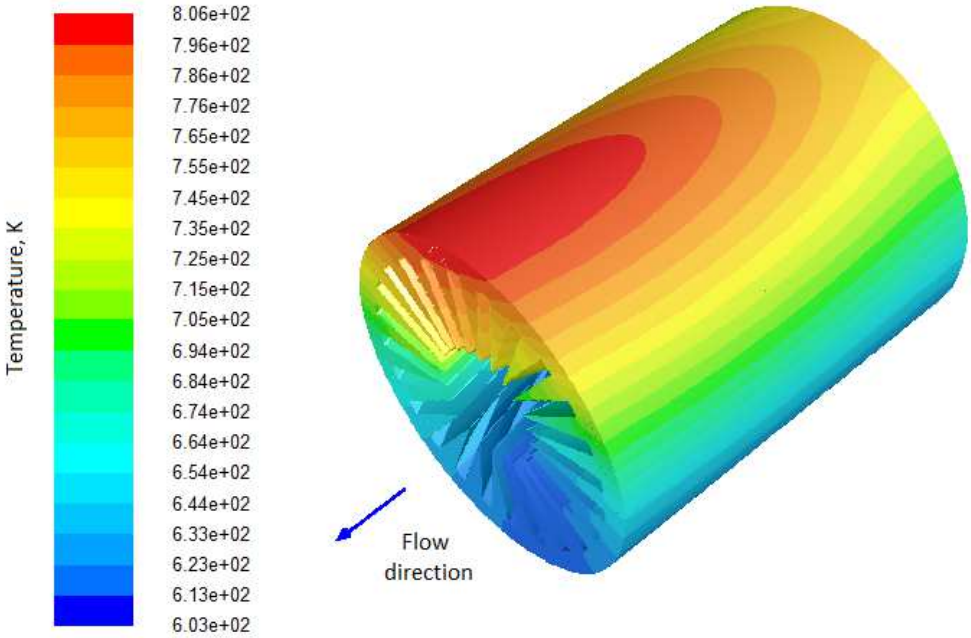

Figure 3. Temperature contour plots on solid surfaces.

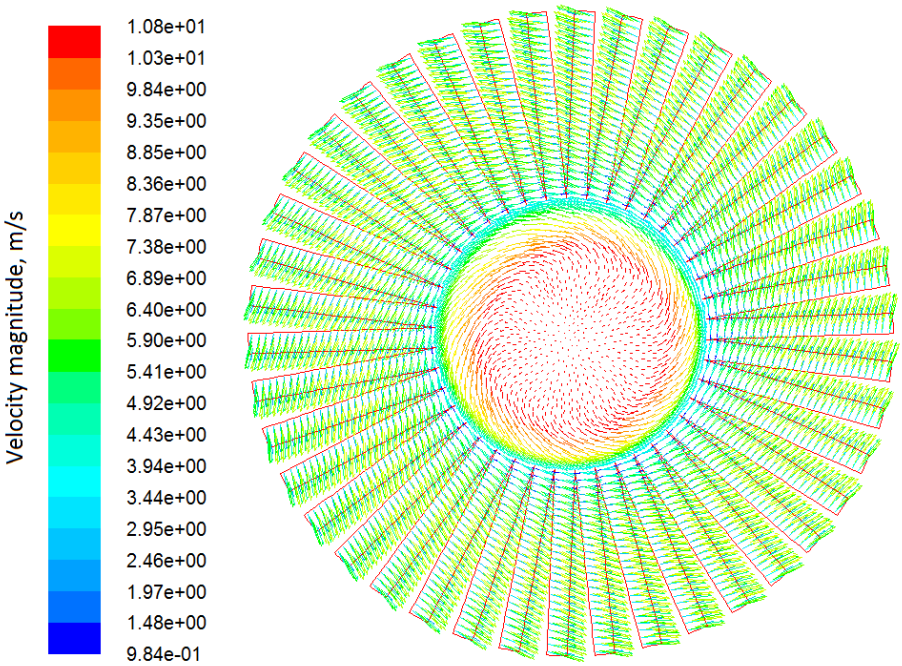

Figure 4 Velocity vectors projected onto the x-y plane (plane of paper) at the outlet boundary.

The gradient vector was calculated using a forward stepping finite difference method.

$$\left.\frac{\partial T}{\partial D^*}\right|_0 \approx \frac{T(D_0+\Delta D, w_0, N_0, t_0, \theta_0) - T(D_0, w_0, N_0, t_0, \theta_0)}{\Delta D / D_{max}}, \text{ etc.}$$

with $\Delta D = 0.01 D_{max}$.

The solution converged to $|D_{n+1} - D_n| \leq 0.005 D_n$ within 6 iterations. Tolerances on all other design variables were well below this criterion. Through optimization, it was possible to reduce the maximum material temperature by almost 65 °C, as shown in table 2. Figure 4 is a graphical presentation of the convergence process.

Iter	D [mm]	w [mm]	N [-]	t [mm]	θ [°]	T [K]
0	20.00	1.00	24	1.60	30	804.76
1	16.00	0.50	44	1.87	45	742.58
2	17.81	0.50	43	1.63	45	740.77
3	16.81	0.61	43	1.54	45	742.11
4	18.26	0.60	42	1.46	45	740.50
5	18.11	0.57	42	1.50	45	740.59
6	18.06	0.57	42	1.50	45	740.57

Table 2 Convergence history of design variables.

Fin helical angle hit its upper limit at the first iteration, and remained there. Tube wall thickness hit its lower limit after four iterations, and remained stuck there for the last three iterations. Gap size first ran up against its lower limit, but then move back into the permissible range. The other two variables only changed marginally between iterations 1 and 6, with tube diameter the only notable exception. The maximum tube temperature drop sharply after the first iteration, but changed only slightly over the last five iterations.

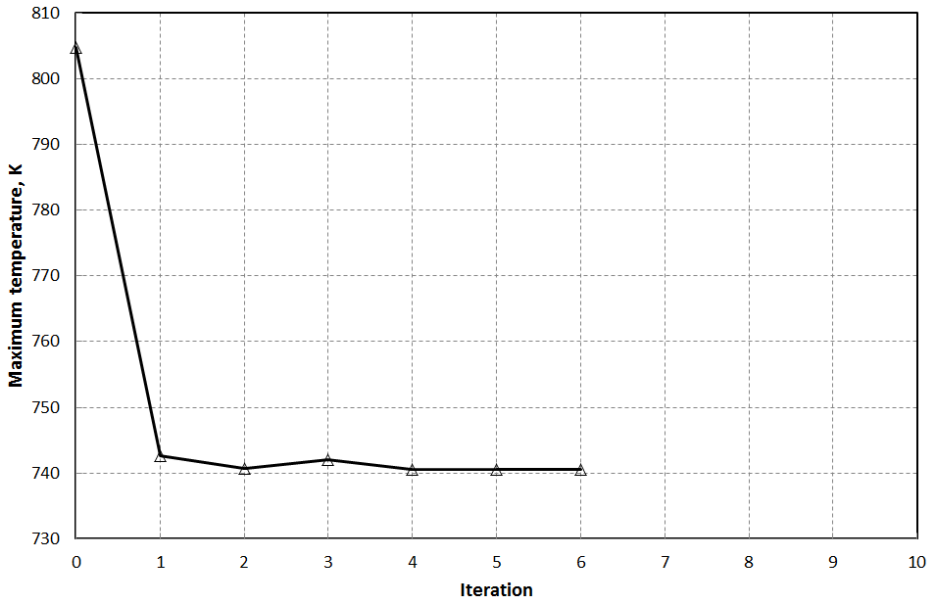

Figure 5. Convergence history of maximum metal temperature.

Finally, a smooth tube with the same internal diameter and wall thickness as the final design was simulated as a reference. The inlet velocity was 5 m/s, the same as for the finned tube. In practice, this may not be realistic in view of the additional flow resistance. The flow in the smooth tube should be turbulent (Re ≈ 14 500), and once again, the shear stress transport k-ω turbulence model was used. The turbulence intensity at the inlet was set to 2 %. The average y^+ on the tube wall was about 7, which is a little on the high side. The maximum temperature recorded for the smooth tube was 1 089.8 K, and the pressure drop 14.4 Pa. Hence, the fins reduced the maximum metal temperature by almost 350 K, but this came at the cost of a tenfold increase in the pressure drop.

5. Conclusion

Tall, triangular fins can reduce the maximum metal temperature in a solar receiver substantially, but it comes at the cost of a tenfold increase in the pressure drop. A further temperature decrease was realized through design optimization. There was a large temperature difference between the top and bottom of the tube, that could lead to high thermal stresses and deformation. Due to the small gaps between the fins, tube deformation may lead to blocking of flow passages between fins. The work presented here has to be expanded to include thermal stress. Other fin configurations need to be explored, as well as different tube materials. For example, by using copper, maximum temperature of the initial design could be lowered by almost 200 K. The thermal conductivity of high temperature materials from the Inconel family increase with temperature, whilst that of steel decrease. That may also drive the outcome of the optimization process in a different direction. Revision of the target function is also required. A more appropriate target function might be to maximize Brayton cycle efficiency, constrained by temperature and stress limits.

References

[1] Kröger, D.G., The **S**tellenbosch **UN**iversity **S**olar **PO**wer **T**hermodynamic cycle, http://blogs.sun.ac.za/sterg/files/2011/05/SUNSPOT-2.pdf.

[2] Kretzschmar, H. and Gauché, Hybrid Pressurized Air Receiver for the SUNSPOT Cycle, Proceedings of the 1st South African Solar Energy Conference, Stellenbosch, 2012.

[3] Kim, J-H., Jansen, K.E. and Jensen, M.K., Analysis of Heat Transfer Characteristics in Internally Finned Tubes, Numerical heat Transfer, Vol. 46, pp. 1 – 21, 2004.

[4] Bazaraa, M.S., Sherali, H.D. and Shetty, C.M., Nonlinear Programming: Theory and Algorithms, 2nd Edition, John Wiley & Sons, Inc., 1993.

[5] Snyman, J.A. and Hay, A.M., The Spherical Quadratic Steepest Descent (SQD) Method for Unconstrained Minimization with no Explicit Line Searches, Computers and Mathematics with Applications, Vol. 42, pp. 169 – 178, 2001.

[6] Groenwold, A.A. Etman, L.F.P. and Wood, D.W., Approximated Approximations for SAO, Structural and Multidisciplinary Optimization, Vol. 41, pp. 39 – 56, 2010.

[7] Holman, J.P., Heat Transfer, 5th Edition, McGraw-Hill, 1981.

[8] Versteeg, H.K. and Malalasekera, W., An Introduction to Computational Fluid Dynamics: The Finite Volume Method, 2nd Edition, Pearson Education Ltd, 2007.

[9] White, F.M., Viscous Fluid Flow, 2nd Edition, McGraw-Hill, 1991.

[10] Roache, P.J., Verification and Validation in Computational Science and Engineering, Hermosa Publishers, 1998.